Composites Part B 180 (2020) 107562

Contents lists available at ScienceDirect

Composites Part B

journal homepage: www.elsevier.com/locate/composites

Controlling toughness and strength of FDM 3D-printed PLA components through the raster layup

Josef Kiendl *, Chao Gao

Department of Marine Technology – Norwegian University of Science and Technology, NO-7491 Trondheim, Norway

ARTICLE INFO

Keywords:
3D printing
Fused Deposition Modeling
Polylactic acid
Strength
Toughness
Material design

ABSTRACT

We investigate the influence of raster layup on the resulting material properties of FDM 3D-printed materials made of PLA. In particular, we investigate the resulting toughness, strength, and stiffness, with a special focus on toughness. We show that for standard layups with layer orientations alternating by 90°, stiffness and strength are almost isotropic, while a strong anisotropy is obtained for toughness. Moreover, we show that materials with such a layup can even switch their behavior from brittle to ductile depending on the loading direction. Finally, we propose a new layer stacking scheme which simultaneously provides increased toughness and increased strength compared to the standard approaches.

1. Introduction

Fused Deposition Modeling (FDM) is a 3D printing technology, where a thermoplastic filament is partially melted and extruded by a heated nozzle, and deposited layer by layer on a build platform [1]. Many different filament materials are available, with Acrylonitrile Butadiene Styrene (ABS) and Polylactic Acid (PLA) being the most common ones. The versatility and the low equipment costs have made FDM the most widespread 3D printing technology today. While it initially was used only for prototyping, it is nowadays shifting towards a manufacturing process for mechanical components, which is also due to the development of filaments from materials with high strength, like Polyether Ether Ketone (PEEK), and fiber-reinforced filaments [2–5]. However, a major obstacle in using this technology for the design of load-bearing components is the fact that the mechanical properties of FDM-printed materials significantly differ from those of the filaments' bulk materials. Due to the process of filament deposition in FDM, each material layer is made up of (mostly parallel) fibers connected to each other by adhesive bonding. The fiber raster orientation can vary from layer to layer, and the standard configuration is a raster change by 90° between layers. The material structure, obtained by this process, is called the mesostructure, and it has been found in several studies that it has a major influence on the resulting mechanical properties of the printed material [6–17]. Most of these studies focused on measuring the material's stiffness and/or strength, and it was found that they depend strongly on the printing direction. Both stiffness and strength were typically found to be highest if the material was loaded in fiber direction, lowest if it was loaded orthogonal to the fibers and somewhere in the middle for composite layups with layer orientations alternating by 90°. While quite a lot of research has been done on the stiffness and strength of FDM components, the relation between the mesostructure and the resulting material toughness appears still unexplored [5,18,19]. Both strength and toughness are important material parameters when it comes to the safe design of load-carrying structures, where strength indicates the maximum load capacity while toughness is a measure for the maximum absorbable energy before failure.

In this paper, we investigate the influence of fiber orientation on the resulting material properties including stiffness, strength, and toughness. We use PLA as base material, which is brittle, and we show that the printed material can result either brittle or ductile which can be controlled by the combination of layer orientations. Furthermore, we show how both strength and toughness can be increased simultaneously by an optimized mesostructural layout.

2. Materials and methods

For printing the test specimens, a Raise3D Pro2 printer and PLA filament by EasyPrint were used. We printed specimens with different raster orientations, both with unidirectional layups and alternating layups. All other print parameters were kept constant for all cases. In particular, we used a layer thickness of 0.2 mm, extruder width of 0.4 mm, and printing speed 30 mm/s to ensure consistent printing quality. Infill density was set to 100% and no contour fibers were used for having uniform properties within the layers. The extruder temperature was set to 200° C, the bed temperature to 60° C. Tensile

* Corresponding author.
E-mail address: josef.kiendl@ntnu.no (J. Kiendl).

https://doi.org/10.1016/j.compositesb.2019.107562
Received 7 June 2019; Received in revised form 11 July 2019; Accepted 24 October 2019
Available online 25 October 2019

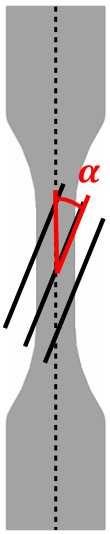

Fig. 1. Layer orientation definition for unidirectional layups.

tests were performed on a Instron mechanical testing machine (Model 8872) with a 25kN load cell at a rate of 0.3 mm/min until failure. The stress–strain curves were calculated based on the initial dimensions of the test samples. All tests were repeated three times, and results are displayed as average values with error bars indicating the standard deviation. Furthermore, digital image correlation (DIC) was used to capture deformation patterns.

3. Results and discussion

The results in this section are structured as follows. First, we investigate specimens with unidirectional layup and different raster orientations. Next, we consider specimens with the standard layup configuration where the raster orientation changes by 90° from layer to layer. Finally, we consider layup configurations with varying relative angles between layers.

3.1. Unidirectional layups

We performed tensile tests for specimens with layups of $[0°]_{10}$, $[45°]_{10}$, and $[90°]_{10}$. The angle describes the printing direction relative to the loading direction, cf. Fig. 1, such that [0°] refers to loading in fiber direction while [90°] refers to loading transverse to the fiber direction, and the subscripts indicate the number of layers. Fig. 2 shows the resulting strain–stress curves as average values together with error bars in (a) and without error bars in (b) for clearer visibility. From this figure, we can directly see that both stiffness and strength depend on the raster angle, which has also been observed in previous studies [6–16]. In particular, it can be seen that both stiffness and strength are highest for 0° and lowest for 90°, and there is a gradual decrease in both parameters for increasing raster angles. Fig. 3(a)–3(b) show the relation between the raster orientation and the resulting Young's modulus E and tensile strength σ_y. Furthermore, we are interested in the resulting toughness Γ, which is obtained as the area under the strain–stress curves. As can be seen in Fig. 3(c), the toughness in unidirectional specimens follows the same general trend as stiffness and strength, having its maximum at 0° and gradually decreasing for increasing orientation angles. Moreover, we note that all cases exhibit rather brittle fracture behavior (according to the fiber's material PLA) with sudden failure after reaching the maximum stress. Fig. 4 shows close-up pictures of the broken specimens. It can be seen that in the 0° case failure happened due to fiber rupture and the crack is oriented orthogonally to the fibers, while in all other cases failure is governed by to fiber debonding and the cracks are oriented with the raster direction.

3.2. 90° alternating layups

Next, we performed tests with layer orientations alternating by 90°, which is the standard setting in most FDM printers. In particular, we tested specimens with $[0°/90°]_5$, $[45°/-45°]_5$, and $[30°/-60°]_5$ layups. The resulting strain–stress curves are depicted in Fig. 5, the obtained values for E, σ_y, and Γ are plotted in Fig. 6. Comparing the different cases, an interesting observation can be made. While stiffness and strength are in the same order of magnitude for all cases, very large differences occur for the toughness. In particular, we obtain an increase in toughness of over 500% when switching from $[0°/90°]_5$ to $[45°/-45°]_5$. It should be noted that both cases represent the same material, just loaded in different directions. Investigating their fracture behavior by means of the strain–stress curves (Fig. 5), we can see that the $[0°/90°]_5$ material exhibits brittle fracture, while the $[45°/-45°]_5$ material has a very ductile behavior with large elongation and softening after the yield point. This behavior is not devoted to real plastic deformation in the filament material, which is very brittle, but rather to changes in the mesostructural layout caused by gradual damage in the fiber-to-fiber bonding. In particular, fibers, which are not parallel or perpendicular to the load direction, undergo a certain rotation reorienting towards the load direction, leading to increased elongation. Indeed, a similar effect can also be observed in the tests on unidirectional layups depicted in Fig. 2, where the $[30°]_{10}$ case results in a higher maximum strain than the $[0°]_{10}$ case. However, in unidirectional layups, this effect of fiber rotation is very limited due to the sudden failure caused by fiber debonding through all layers. Alternating layups prevent such a failure and provide additional resilience enabling significant fiber rotation, which finally results in increased elongation. This effect of fiber rotation can obviously not occur if the fibers are parallel or perpendicular to the load direction, which is the reason why the $[0°/90°]_5$ material exhibits a brittle failure behavior and the lowest toughness. By close inspection of the specimens after the tests, we could observe two different effects of fiber rotation. First, we could measure small rotations of the fibers towards the load

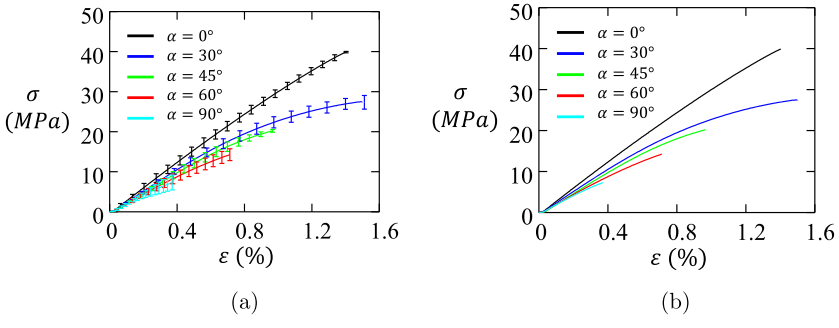

Fig. 2. Test results for unidirectional specimens with different raster angles, average values with errors bars (a) and without errors bars (b).

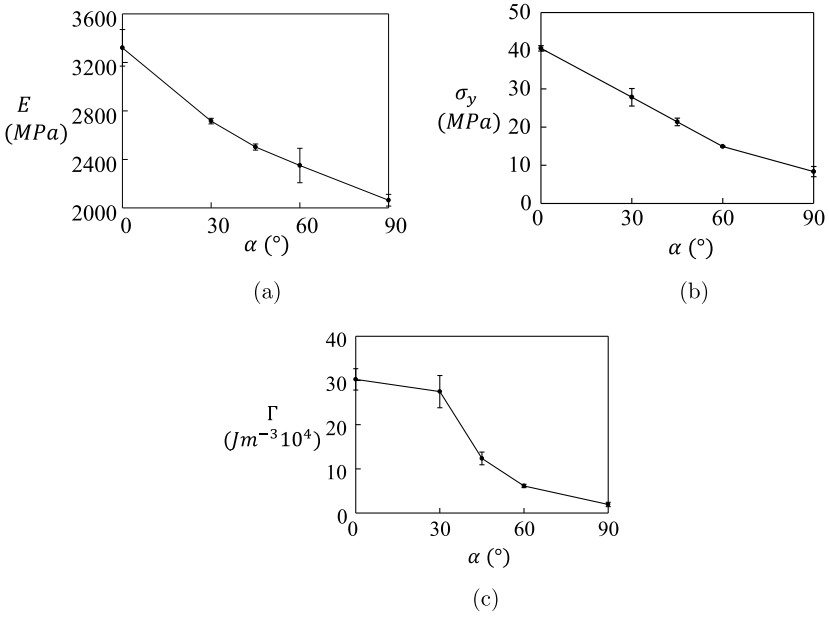

Fig. 3. Dependence of Young's modulus (a), tensile strength (b), and toughness (c) on the raster orientation for unidirectional specimens.

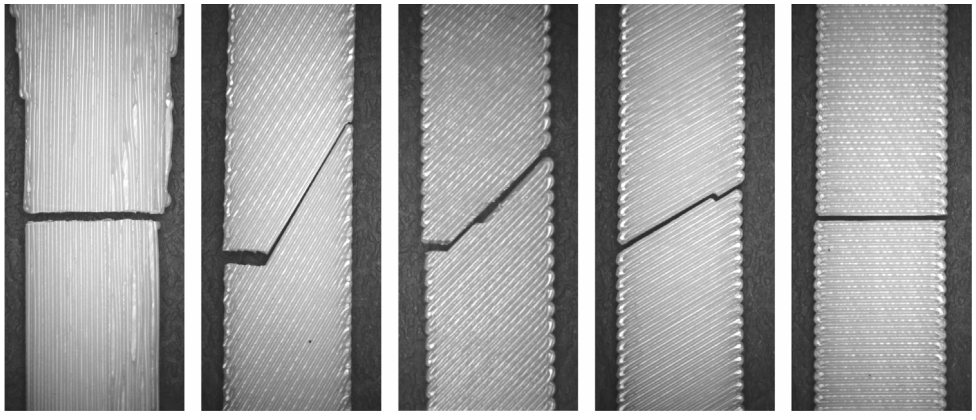

Fig. 4. Unidirectional specimens with different raster angles after failure.

direction all over the specimen, and second, there are short sections of fibers within the cracks, which have completely oriented with the load direction before they ruptured, as shown in the close-up pictures in Fig. 7. For measuring the rotation of the fibers outside the crack, we used digital image correlation. We measured the rotation at three different points placed outside the regions which are largely deformed due to the crack, and averaged them. Table 1 reports the measured rotations for the samples shown in Fig. 7. For better understanding the damage evolution in the specimens, we also tracked their deformation during the tests. Fig. 8 depicts snapshots of a $[45°/-45°]_5$ specimen at different time instants corresponding to different points in the strain–stress curves.[1] We can observe that right after "yielding" and also for large regions of the "softening" regime there is no visible damage in the specimen. This indicates that at these deformation levels, damage occurs mainly in the fiber bonding but not in the fibers themselves, leading to the effect of fiber rotation discussed above. Only shortly before the point of rupture, we can observe the formation of two lines of fiber damage, which run orthogonal to the fibers in the visible layer, i.e., they are parallel to the bonding lines in the layer underneath. Along these lines the fibers in the top layer (and all the layers with the same orientation) start to yield and rupture which finally initiates cracking and failure of the specimen.

Table 1
Average fiber rotation at final deformation stage for different layups.

Layup	$[45/-45°]_5$	$[30°/-60°]_5$	$[0°/90°]_5$
Average fiber rotation	1.7°	0.8°	0.0°

3.3. Symmetrically-aligned alternating layups

The results in the previous sections showed that strength and toughness of the printed material can be controlled by the layer stacking sequence, where a unidirectional $[0°]_{10}$ layup provides the highest strength but with low toughness, while alternating layups result in lower strength but highly increased toughness if oriented inclined to the loading direction. Based on these findings, we now investigate a

[1] It may be noted that the strain–stress curve of the $[45°/-45°]_5$ case in Fig. 5 is different than the curve in Fig. 8 This is because the former shows averaged results, while the latter depicts the results of one specific case.

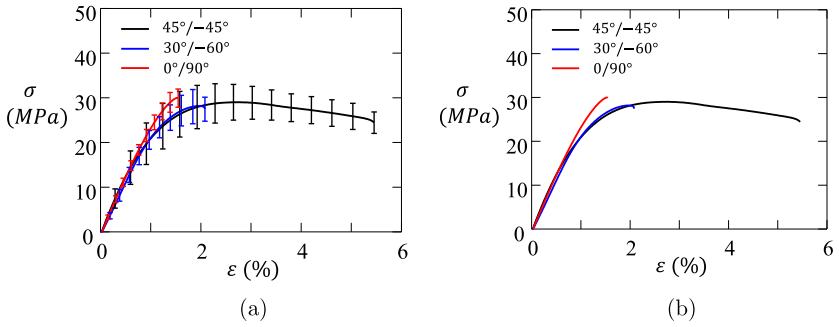

Fig. 5. Test results for specimens with layer orientations alternating by 90°, average values with errors bars (a) and without errors bars (b).

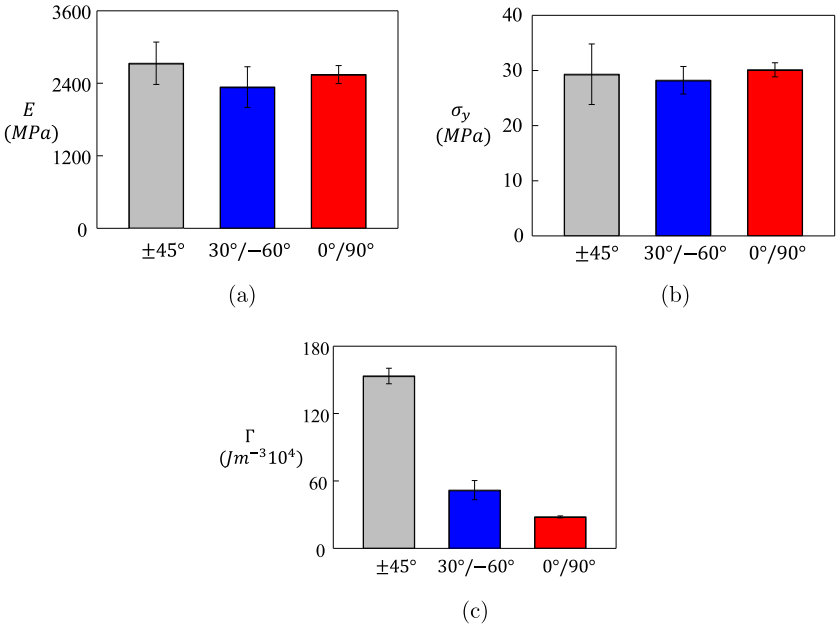

Fig. 6. Young's modulus (a), tensile strength (b), and toughness (c) for different alternating layups.

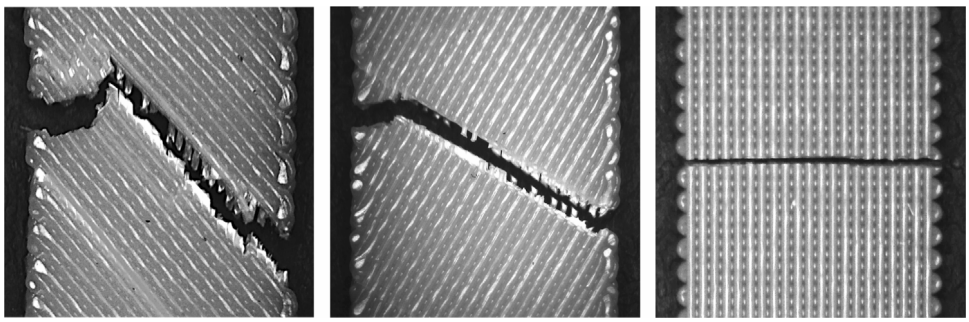

(a) $[45°/-45°]_5$ (b) $[30°/-60°]_5$ (c) $[0°/90°]_5$

Fig. 7. Specimens with layer orientations alternating by 90° after failure.

different layer stacking scheme with the aim of obtaining high strength and high toughness simultaneously. Instead of alternating layer orientations by 90°, we orient them as $[\beta/-\beta]_5$, where β is measured towards the loading direction, see Fig. 9. The idea behind this approach is that for small β angles, we may obtain high strength values close to the $[0°]_{10}$ case but with increased toughness due to the possibility that fibers undergo a certain rotation before rupture. We performed studies for different β values ranging from 0° to 90°, and the resulting strain–stress curves are depicted in Fig. 10 (for better clarity of the figure, error bars are omitted in this plot). Furthermore, the relations between β and the resulting values for stiffness, strength, and toughness are plotted in Fig. 11. We note that $\beta = 0°$ and $\beta = 90°$ represent the unidirectional layups $[0°]_{10}$ and $[90°]_{10}$, respectively. In these two cases, the material behaves almost perfectly brittle, while a certain ductility can be observed for all other cases, and there is a continuous transition from brittle to ductile back to brittle with increasing β. Furthermore,

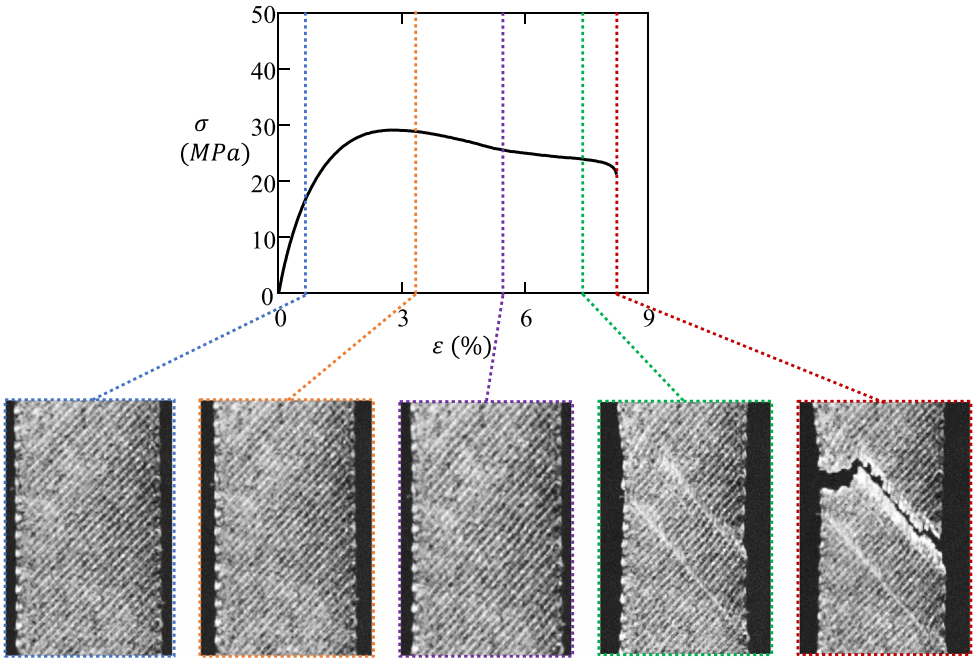

Fig. 8. Snapshots of a $[45°/-45°]_5$ specimen at different strain levels.

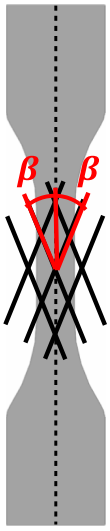

Fig. 9. Proposed scheme for alternating layups.

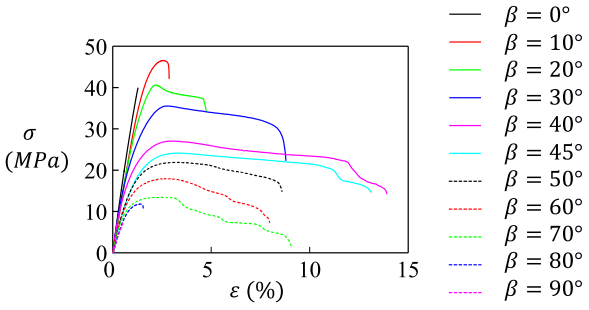

Fig. 10. Strain–stress curves for layups with different β.

it is interesting to note that the highest strength is not obtained for $\beta = 0°$ but for $\beta = 10°$. Compared to the unidirectional case, it exhibits an increase in strength of 17% and an increase in toughness of 281%. With $\beta = 20°$ the strength is similar to the unidirectional case (increase of 2%) but toughness is increased by 340%. The maximum toughness is obtained for $\beta = 40°$ with an increase of 462% compared to the unidirectional case, but with a reduction of strength by 15%. From these results, we may conclude that all layups with $10° \leq \beta \leq 40°$ produce materials with optimized combinations of strength and toughness.

4. Conclusions

We investigated mechanical properties, in particular toughness, strength, and stiffness, of FDM 3D-printed specimens made of PLA. We found that for unidirectional layups, all toughness, strength, and stiffness are highest if the fibers are aligned with the loading direction. For layups with layer orientations shifted by 90°, which is the standard in FDM printing, we found that the material is quite isotropic in terms of stiffness and strength, but not at all in terms of toughness. In particular, we found that the material exhibits much higher toughness when loaded diagonally to the raster compared to loading parallel/perpendicular to the raster. Moreover, we found that the principal material behavior changes with the loading direction, from brittle for parallel loading to ductile for inclined loading. These effects are devoted to the fact that damage initiates in the inter-fiber bonding, which allow fibers to rotate and reorient towards the load direction, leading to significantly increased elongation before rupture. Based on these findings, we investigated a new layer staggering scheme with alternating layers aligned symmetrically with respect to the loading direction, indicated by $[\beta/-\beta]_5$. With this scheme, we could obtain optimized material performance providing high strength and high toughness simultaneously. We note that the above-mentioned results refer to uniaxial load conditions. As part of our future research we want to extend these studies to multiaxial loading, considering helicoidal fiber architectures which have been found to provide highly improved damage tolerance in the cuticles of different animals [20,21]. Finally, the results of this experimental study are an important basis for developing numerical approaches for the modeling and simulation

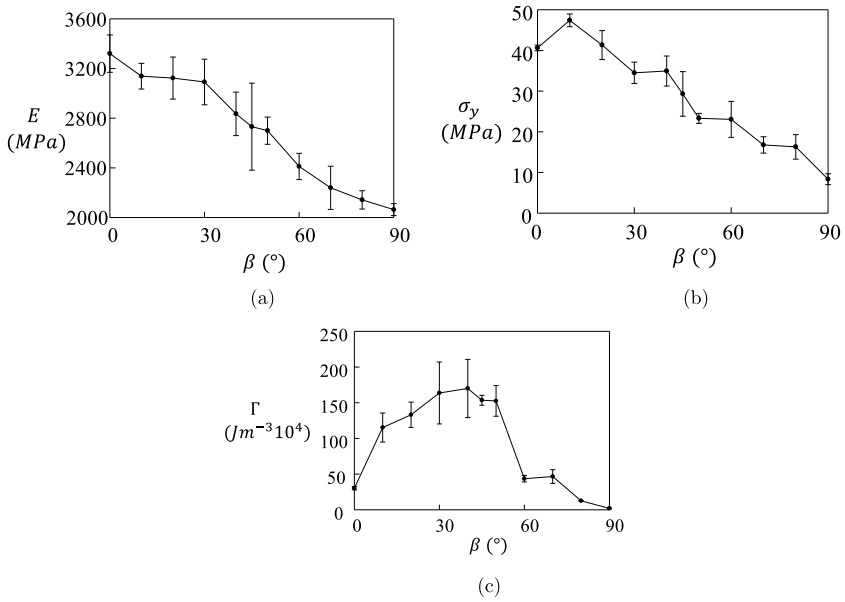

Fig. 11. Dependence of Young's modulus (a), tensile strength (b), and toughness (c) on β.

of FDM materials. So far, most researchers considered FDM materials as composite laminates and used classical lamination theory for its analysis [9,11,22,23], where the validity is restricted to linear elastic analysis. In [7], the authors used classical laminate theory together with a Tsai–Hill yielding criterion for predicting the strength of unidirectional ABS specimens. Although good results were obtained for the unidirectional cases, we believe that such homogenizing approaches cannot predict accurately the complex mechanical behavior in alternative layups observed in our studies, which are driven by local effects (like partial debonding and fiber rotation) at the mesoscale. The development of modeling approaches taking into account these effects is planned as further research.

Acknowledgment

J. Kiendl was supported by the Onsager fellowship program of the Norwegian University of Science and Technology (NTNU). This support is gratefully acknowledged.

References

[1] Ngo TD, Kashani A, Imbalzano G, Nguyen KTQ, Hui D. Additive manufacturing (3D printing): A review of materials, methods, applications and challenges. Composites B 2018;143:172–96.
[2] Goh GD, Yap YL, Agarwala S, Yeong WY. Recent progress in additive manufacturing of fiber reinforced polymer composite. Adv Mater Technol 2019;4(1):1–22.
[3] Quan Z, Wu A, Keefe M, Qin X, Yu J, Suhr J, et al. Additive manufacturing of multi-directional preforms for composites: Opportunities and challenges. Mater Today 2015;18(9):503–12.
[4] Parandoush P, Lin D. A review on additive manufacturing of polymer-fiber composites. Compos Struct 2017;182:36–53.
[5] Brenken B, Barocio E, Favaloro A, Kunc V, Pipes RB. Fused filament fabrication of fiber-reinforced polymers: A review. Addit Manuf 2018;21:1–16.
[6] Ahn S-H, Montero M, Odell D, Roundy S, Wright PK. Anisotropic material properties of fused deposition modeling ABS. Rapid Prototyp J 2002;8(4):248–57.
[7] Alaimo G, Marconi S, Costato L, Auricchio F. Influence of meso-structure and chemical composition on FDM 3D-printed parts. Composites B 2017;113:371–80.
[8] Bellini A, Güçeri S. Mechanical characterization of parts fabricated using fused deposition modeling. Rapid Prototyp J 2003;9(4):252–64.
[9] Li L, Sun Q, Bellehumeur C, Gu P. Composite modeling and analysis for fabrication of FDM prototypes with locally controlled properties. J Manuf Process 2002;4(2):129–41.
[10] Li H, Wang T, Sun J, Yu Z. The effect of process parameters in fused deposition modelling on bonding degree and mechanical properties. Rapid Prototyp J 2018;24(1):80–92.
[11] Kulkarni P, Dutta D. Deposition strategies and resulting part stiffnesses in fused deposition modeling. J Manuf Sci Eng 1999;121(1):93.
[12] Es-Said OS, Foyos J, Noorani R, Mendelson M, Marloth R, Pregger BA. Effect of layer orientation on mechanical properties of rapid prototyped samples, materials and manufacturing processes. Mater Manuf Process 2010;15(1):107–22.
[13] Wu W, Geng P, Li G, Zhao D, Zhang H, Zhao J. Influence of layer thickness and raster angle on the mechanical properties of 3D-printed PEEK and a comparative mechanical study between PEEK and ABS. Materials 2015;8(9):5834–46.
[14] Mohamed OA, Masood SH, Bhowmik JL. Experimental investigation of time-dependent mechanical properties of PC-ABS prototypes processed by FDM additive manufacturing process. Mater Lett 2017;193:58–62.
[15] Popescu D, Zapciu A, Amza C, Baciu F, Marinescu R. FDM Process parameters influence over the mechanical properties of polymer specimens: A review. Polym Test 2018;69:157–66.
[16] Lee CS, Kim SG, Kim HJ, Ahn SH. Measurement of anisotropic compressive strength of rapid prototyping parts. J Mater Process Technol 2007;187–188:627–30.
[17] Garg A, Bhattacharya A. An insight to the failure of FDM parts under tensile loading: finite element analysis and experimental study. Int J Mech Sci 2017;120:225–36.
[18] Goh GD, Yap YL, Tan HKJ, Sing SL, Goh GL, Yeong WY. Process-structure-properties in polymer additive manufacturing via material extrusion: A review. Crit Rev Solid State Mater Sci 2019;1–21.
[19] Mohamed OA, Masood SH, Bhowmik JL. Optimization of fused deposition modeling process parameters: a review of current research and future prospects. Adv Manuf 2015;3(1):42–53.
[20] Weaver JC, Milliron GW, Miserez A, Evans-Lutterodt K, Herrera S, Gallana I, et al. The stomatopod dactyl club: A formidable damage-tolerant biological hammer. Science 2012;336:1275–80.
[21] Zaheri A, Fenner J, Russell B, Restrepo D, Daly M, Wang D, et al. Revealing the mechanics of helicoidal composites through additive manufacturing and beetle developmental stage analysis. Adv Funct Mater 2018;28(1803073).
[22] Rodríguez JF, Thomas JP, Renaud JE. Mechanical behavior of acrylonitrile butadiene styrene fused deposition materials modeling. Rapid Prototyp J 2003;9(4):219–30.
[23] Somireddy M, Czekanski A, Singh CV. Development of constitutive material model of 3D printed structure via FDM. Mater Today Commun 2018;15:143–52.